

# Lawrence Berkeley National Laboratory

## LBL Publications

### Title

Magnetic Field Quality Analysis Using ANSYS

### Permalink

<https://escholarship.org/uc/item/5xf0t10g>

### Authors

Dell'Orco, D

Chen, Y

### Publication Date

1991-03-01



# Lawrence Berkeley Laboratory

UNIVERSITY OF CALIFORNIA

## Accelerator & Fusion Research Division

To be presented at the 1991 ANSYS Conference and  
Exhibition, Pittsburgh, PA, May 21-23, 1991, and to be  
published in the Proceedings

### Magnetic Field Quality Analysis Using ANSYS

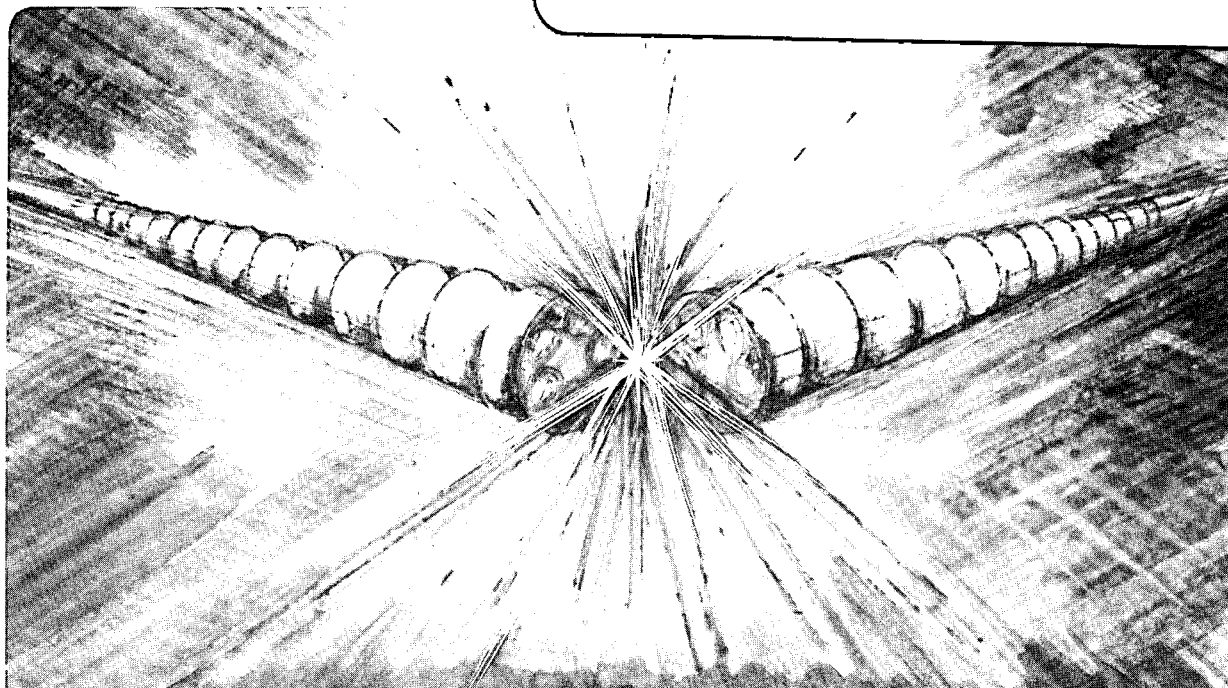
D. Dell'Orco and Y. Chen

March 1991

*U. C. Lawrence Berkeley Laboratory  
Library, Berkeley*

# FOR REFERENCE

Not to be taken from this room



Copy 1  
Bldg. 50 Library.

LBL-30455

## **DISCLAIMER**

This document was prepared as an account of work sponsored by the United States Government. While this document is believed to contain correct information, neither the United States Government nor any agency thereof, nor the Regents of the University of California, nor any of their employees, makes any warranty, express or implied, or assumes any legal responsibility for the accuracy, completeness, or usefulness of any information, apparatus, product, or process disclosed, or represents that its use would not infringe privately owned rights. Reference herein to any specific commercial product, process, or service by its trade name, trademark, manufacturer, or otherwise, does not necessarily constitute or imply its endorsement, recommendation, or favoring by the United States Government or any agency thereof, or the Regents of the University of California. The views and opinions of authors expressed herein do not necessarily state or reflect those of the United States Government or any agency thereof or the Regents of the University of California.

## Magnetic Field Quality Analysis Using ANSYS\*

Domenico Dell'Orco and Yanping Chen  
Lawrence Berkeley Laboratory  
University of California  
Berkeley, CA 94720

### ABSTRACT

The design of superconducting magnets for particles accelerators requires a high quality of the magnetic field. This paper presents an ANSYS 4.4A Post1 macro that computes the field quality performing a Fourier analysis of the magnetic field.

The results show that the ANSYS solution converges toward the analytical solution and that the error on the multipole coefficients depends linearly on the square of the mesh size. This shows the good accuracy of ANSYS in computing the multipole coefficients.

### INTRODUCTION

The design of superconducting magnets for particle accelerators requires a Fourier analysis of the magnetic field in order to evaluate the field quality. Since ANSYS 4.4A does not have such a built-in capability, we have developed and tested an internal routine that does it. We have considered three different configurations of particle accelerator magnets and have performed an error analysis. The element used in this magnetic linear analysis is STIF 13 [1] and the element shape used is quadrilateral. The results show that the ANSYS results converge toward the analytical solution and that the error on the multipole coefficients depends linearly on the square of the mesh size. We have also found that the automatic meshing introduces small errors in the geometry of the problem and makes the results converge to a slightly different solution. This problem can be corrected by modifying the nodes locations with the NMODIF command.

The configurations considered for this test are one dipole and two quadrupole magnets with  $\cos(n\theta)$  geometry (see Figures 1 and 2). A perfect dipole magnet gives a uniform field in the magnet bore in order to bend the particles, where as a quadrupole magnet has a field that depends linearly on the radius and by the cosine of the azimuthal angle.

The Fourier analysis of the magnetic flux density is performed along a circumference ( $r=10$  mm) concentric with the center of the beam particle. A perfect  $n$ -pole magnet has only one fundamental multipole component. In reality since the current flows in cables of simple cross section shape, the magnets will always have multipole components other than the fundamental. One part of the magnetic design of a superconducting magnet consists in minimizing the unwanted multipole components of the field by varying the layout of the cables.

The multipole components are measured in  $T/cm^{(n-1)}$  where  $n$  is the order of the multipole component ( $n=1$  for dipole,  $n=2$  for quadrupole,  $n=3$  for sextupole,...). The ratio of the secondary components to the fundamental must be kept within the specification of the magnet, normally less than  $10^{-4}$ . This means that a dipole magnet with central field of 1 T should have all the secondary multipole components less than  $10^{-4} T/cm^{(n-1)}$  while the error in the numerical computation should be  $\sim 10^{-5} T/cm^{(n-1)}$ .

\*This work was supported by the Director, Office of Energy Research, Office of High Energy and Nuclear Physics, Division of High Energy Physics, of the U.S. Department of Energy under Contract No. DE-AC03-76SF00098.

## NUMERICAL FORMULATION

The magnetic field can be described in the following way:

$$F = B_y + i B_x = \sum_{i=1}^{\infty} (b_n + i a_n) r^{n-1} e^{i(n-1)\theta} \quad \text{eq.(1)}$$

where B is the magnetic flux density, r the radius at which the multipole analysis is performed,  $\theta$  the azimuthal angle on the circumference,  $a_n$  the skew multipole component and  $b_n$  the normal multipole component. From equation 1 it is derived:

$$a_n = \frac{-1}{2\pi} \int_0^{2\pi} [B_x \cos(n-1)\theta - B_y \sin(n-1)\theta] r^{1-n} d\theta \quad \text{eq.(2)}$$

$$b_n = \frac{-1}{2\pi} \int_0^{2\pi} [B_y \cos(n-1)\theta - B_x \sin(n-1)\theta] r^{1-n} d\theta \quad \text{eq.(3)}$$

Considering the definition of the magnetic vector potential  $\phi$ :

$$B_r = \frac{1}{r} \frac{\partial \phi}{\partial \theta} \quad B_\theta = -\frac{\partial \phi}{\partial r} \quad \text{eq.(4)}$$

and supposing that the vector potential depends linearly on  $\theta$ , equations 2-3 can be evaluated numerically in the following way:

$$a_n = \frac{-1}{n\pi r^n} \sum_i \frac{\Delta \phi_i}{\Delta \theta_i} (\sin n\theta_i - \sin n\theta_{i-1}) \quad \text{eq.(5)}$$

$$b_n = \frac{1}{n\pi r^n} \sum_i \frac{\Delta \phi_i}{\Delta \theta_i} (\cos n\theta_i - \cos n\theta_{i-1}) \quad \text{eq.(6)}$$

where i is the node number along the circumference of radius r,  $\Delta \phi_i = \phi_i - \phi_{i-1}$  and  $\Delta \theta_i = \theta_i - \theta_{i-1}$ .

The normal multipole components  $b_n$  are evaluated directly in POST1 using the routine listed in the appendix. This method of computing the multipole coefficients has the advantage of using directly the magnetic vector potential and not the flux density B, obtained by differentiating it. The routine in the appendix avoids the transfer of ANSYS results to an external software (or to the PREP6 in which it is also possible to perform a Fourier analysis).

## DESCRIPTION OF THE TEST

We have carried out the test of the routine presented in the appendix for three different magnet configurations:

- a) Dipole magnet with inner radius  $r_1=20$  mm, outer radius  $r_2=40$  mm and  $\theta=56^\circ$  (see Figure 1), no automatic meshing.
- b) Dipole magnet with inner radius  $r_1=20$  mm, outer radius  $r_2=40$  mm and  $\theta=56^\circ$  (see Figure 1), automatic meshing.
- c) Quadrupole magnet with inner radius  $r_1=20$  mm, outer radius  $r_2=40$  mm and  $\theta=20^\circ$  (see Figure 2), no automatic meshing.
- d) Quadrupole magnet with inner radius  $r_1=20$  mm, outer radius  $r_2=40$  mm and  $\theta=34^\circ$  (see Figure 2), no automatic meshing.

In all these four configurations the overall current density in the coils is  $J=400 \text{ A/mm}^2$  and the radius of the circular iron yoke is  $R=45 \text{ mm}$ .

In Figures 1 and 2 it is shown one fourth of the cross section of each magnet. In the case of the two quadrupole magnets we could also have studied only one eighth of the magnet but we did not do it in order to check numerical asymmetries.

The element used in this magnetic linear analysis is STIF 13, and the element shape used is quadrilateral.

The error analysis has been performed varying the mesh size. In Figures 3 and 4 the meshes are shown when the mesh size is arbitrarily considered equal to 1. The mesh sizes used are: 2, 4/3, 1, 2/3, 0.5, 2/5, 1/3.

Since we suppose that the iron has infinite permeability, Neumann boundary conditions have been imposed at the radius  $R$ . The boundary conditions are shown in Figures 1 and 2.

The Fourier analysis has been performed at the radius  $r=10 \text{ mm}$ .

## ANALYTICAL SOLUTION

The analytical solutions for the magnets, considered in Figures 1 and 2, are the following [2]:

$$a_n = 0, \quad b_n = c_n + d_n \quad \text{eq.(7)}$$

In the dipole  $c_n$  and  $d_n$  are the following:

$$c_n = 2 \frac{\mu_0}{\pi} J \frac{r_2^{2-n} - r_1^{2-n}}{n(2-n)} \sin n\theta \quad \text{for } n=1, 3, 5, 7, \dots \quad \text{eq.(8)}$$

$$d_n = 2 \frac{\mu_0}{\pi} \frac{J}{R^{2n}} \frac{r_2^{2+n} - r_1^{2+n}}{n(2+n)} \sin n\theta \quad \text{for } n=1, 3, 5, 7, \dots \quad \text{eq.(9)}$$

In the quadrupole  $c_n$  and  $d_n$  are the following:

$$c_2 = 2 \frac{\mu_0}{\pi} J \ln \frac{r_2}{r_1} \sin 2\theta \quad \text{eq.(10)}$$

$$c_n = 4 \frac{\mu_0}{\pi} J \frac{r_2^{2-n} - r_1^{2-n}}{n(2-n)} \sin n\theta \quad \text{for } n=6, 10, 14, \dots \quad \text{eq.(11)}$$

$$d_n = 4 \frac{\mu_0}{\pi} \frac{J}{R^{2n}} \frac{r_2^{2+n} - r_1^{2+n}}{n(2+n)} \sin n\theta \quad \text{for } n=2, 6, 10, 14, \dots \quad \text{eq.(12)}$$

## RESULTS

In Figures 5-8 the flux lines of the magnetic flux density are shown for three magnet configurations considered.

In Tables 1-4 the multipole components versus the mesh size for the four configurations considered are shown, and in Figures 9-16 the error on the multipole coefficients versus the mesh size square is plotted. In these tables it is also shown the CPU time in seconds required to run the problem on a Sun Sparcstation I and the number of elements contained in each model.

In Figures 9-16 it is shown that all the multipole coefficients depend linearly on the square of the mesh size and that the results converge to the theoretical solution. It is possible to compute very accurately the multipole coefficients by using two different mesh sizes not very refined and then extrapolating the results.

In Figures 11 and 12 it is shown that, since the automatic meshing introduces small error in the geometry (the arc lines are substituted by spline curves), the numerical solution does not converge to the theoretical solution but it has a small error. This problem can be corrected by modifying the nodes locations with the NMODIF command after using the automatic meshing.

Since an accelerator type magnet normally has the ratio of the secondary multipoles to the fundamental less than  $10^{-4}$ , the accuracy required to the analysis is  $\sim 10^{-5}$ . In the dipole example (mesh size = 1/3), the error on all the multipoles is less than  $10^{-5}$  T/cm<sup>(n-1)</sup> and the fundamental is  $b_1 = 7.75$  T.

These results show that ANSYS can be used in computing the magnetic field quality with as good an accuracy as other software specifically designed for magnetic analysis.

## REFERENCES

- [1] De Salvo, G.J., and Gorman, R. W., "ANSYS User's Manual", Rev. 4.4, Swanson Analysis Systems, Inc., Houston PA, (1989).
- [2] R. Perin, Academic Training Programme 1984-1985, Superconducting Components for Accelerators, CERN-European Center for Particle Research.

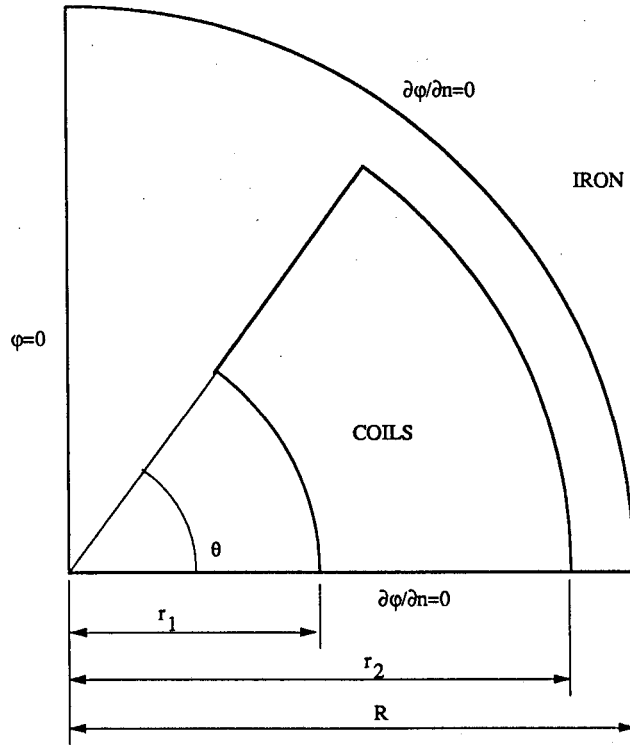


Fig. 1. Dipole magnet cross section and boundary conditions.

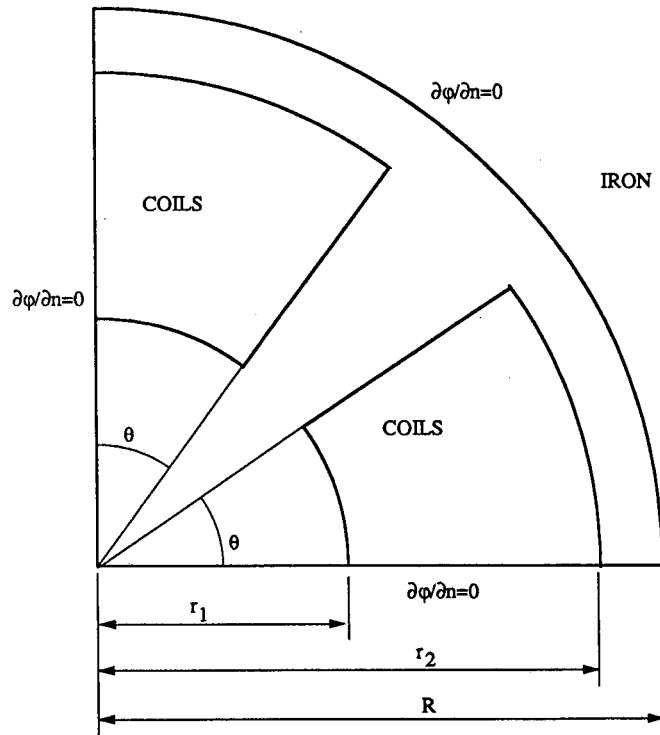


Fig. 2. Quadrupole magnet cross section and boundary conditions.



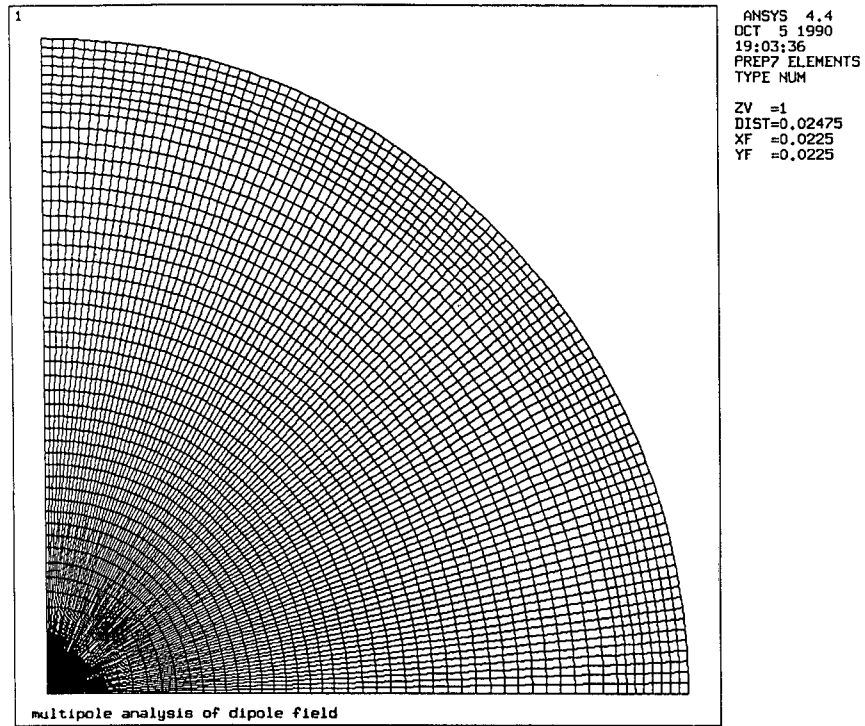


Fig. 3. ANSYS mesh (size=1) for the dipole magnet.

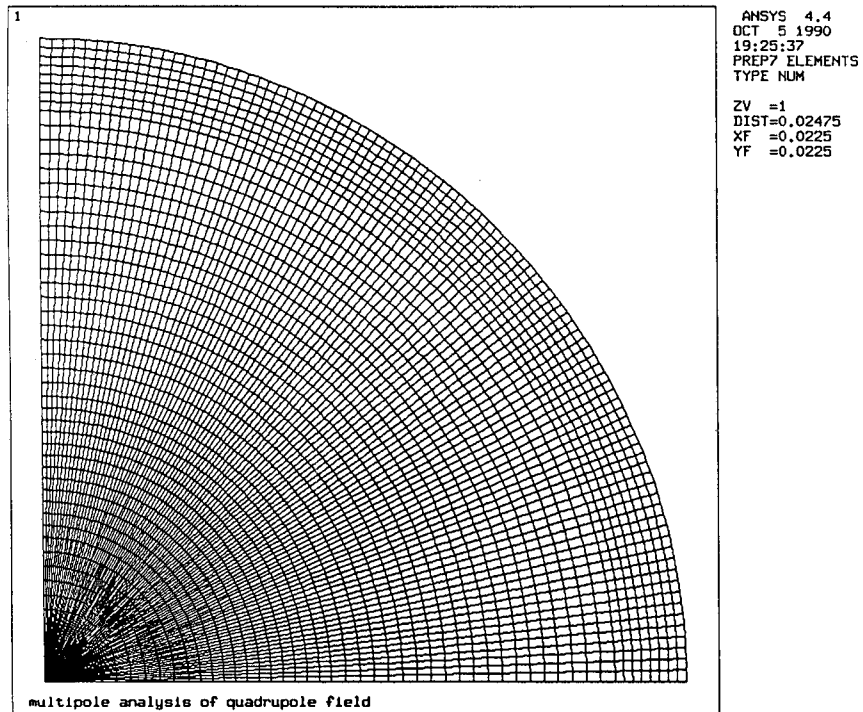


Fig. 4. ANSYS mesh (size=1) for the quadrupole magnet with  $\theta=20^\circ$ .

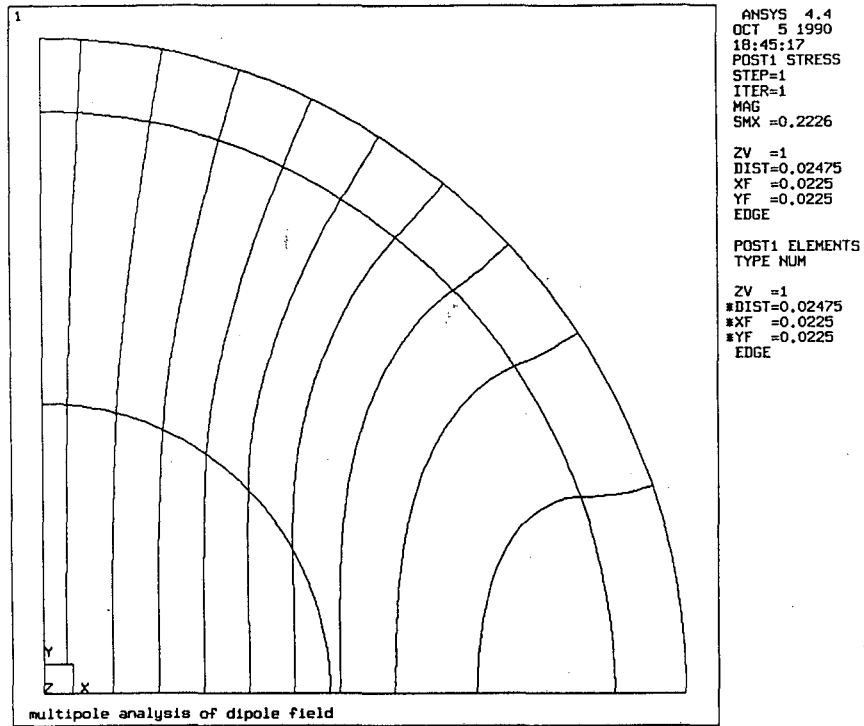


Fig. 5. Flux lines of the magnetic flux density for the dipole.

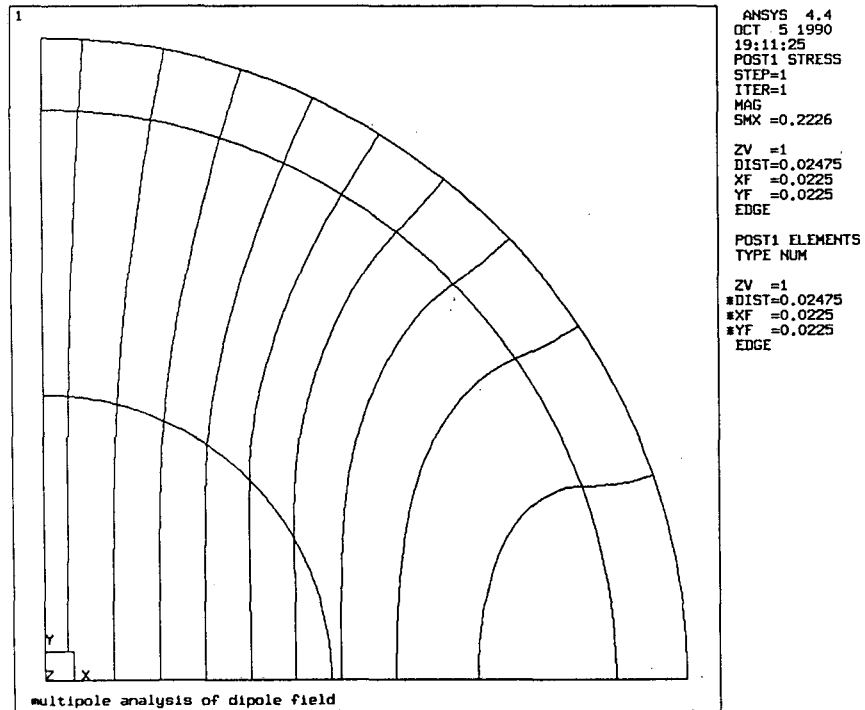


Fig. 6. Flux lines of the magnetic flux density for the dipole with automatic meshing.

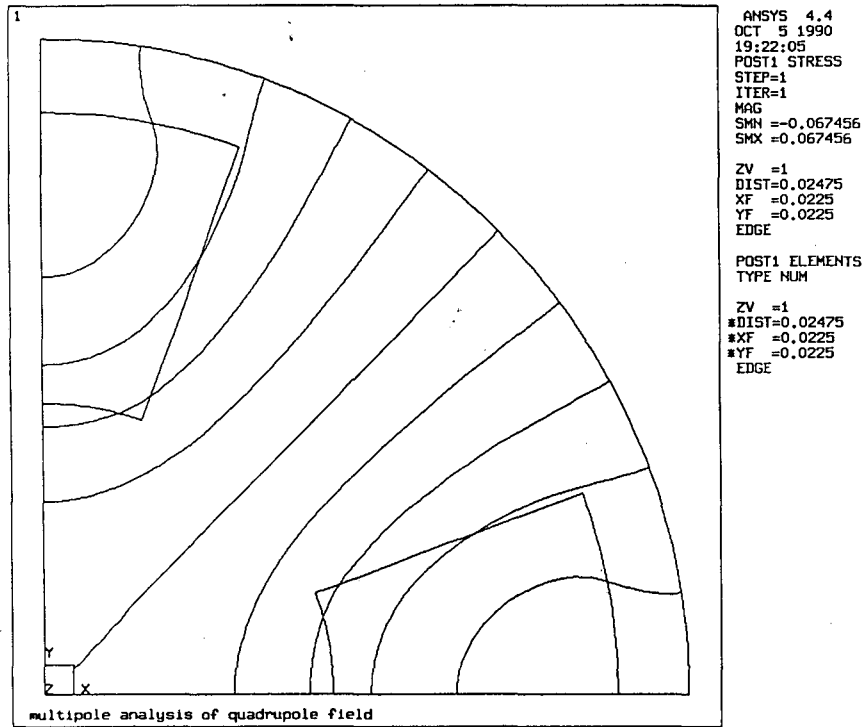


Fig. 7. Flux lines of the magnetic flux density for the quadrupole with  $\theta=20^\circ$ .

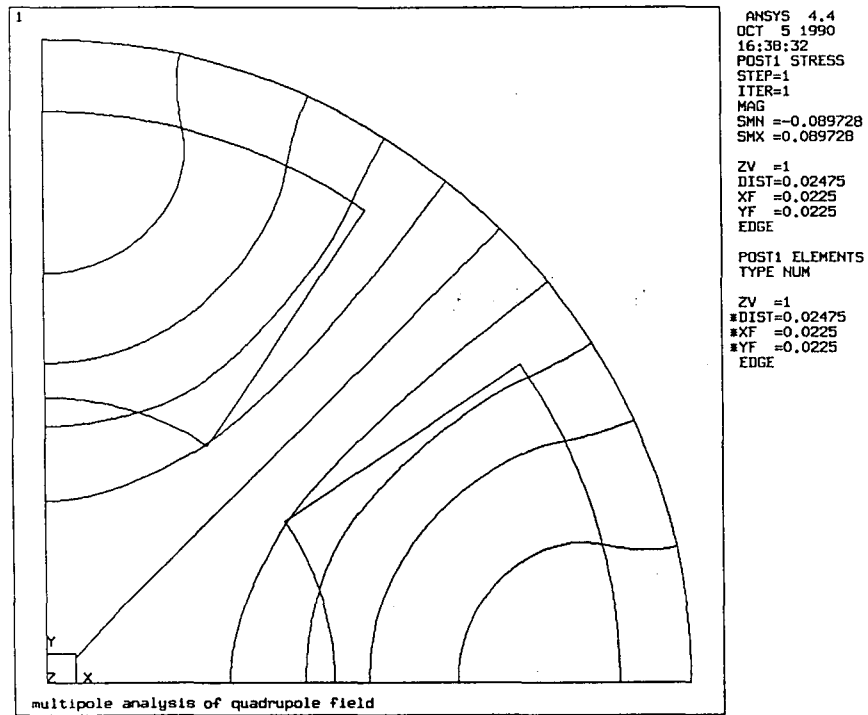


Fig. 8. Flux lines of the magnetic flux density for the quadrupole with  $\theta=20^\circ$ .

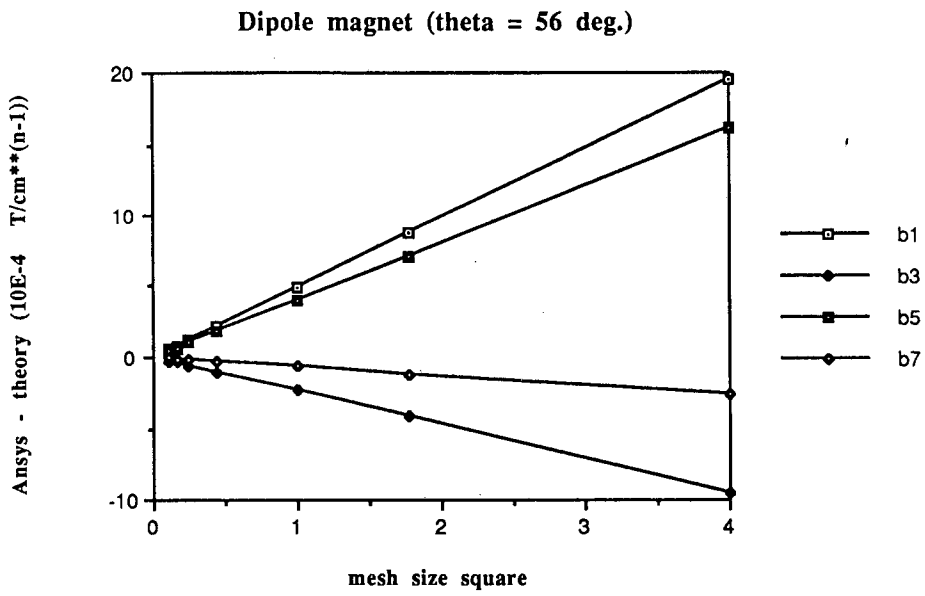


Fig. 9. Multipole coefficients versus mesh size for the dipole.

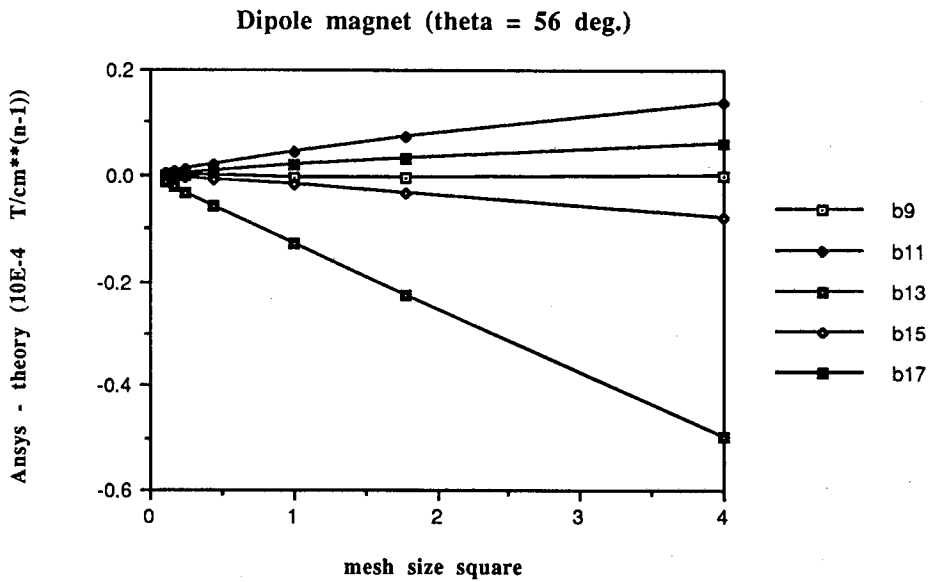


Fig. 10. Multipole coefficients versus mesh size for the dipole.

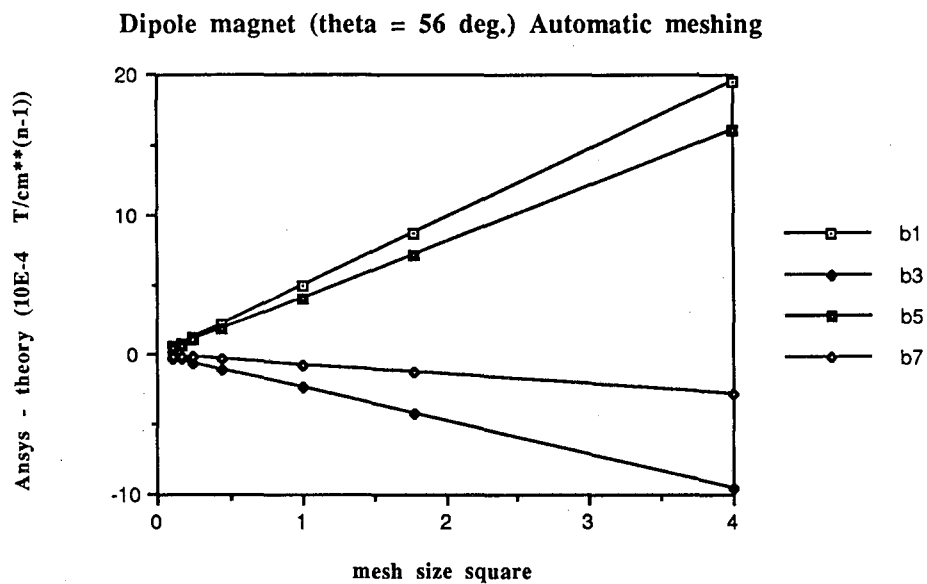


Fig. 11. Multipole coefficients versus mesh size for the dipole with automatic meshing.

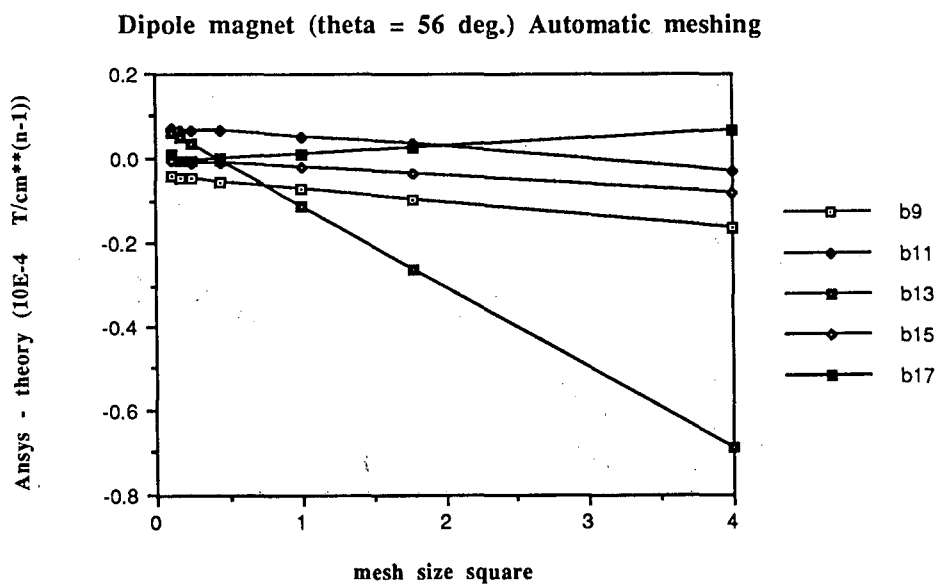


Fig. 12. Multipole coefficients versus mesh size for the dipole with automatic meshing.

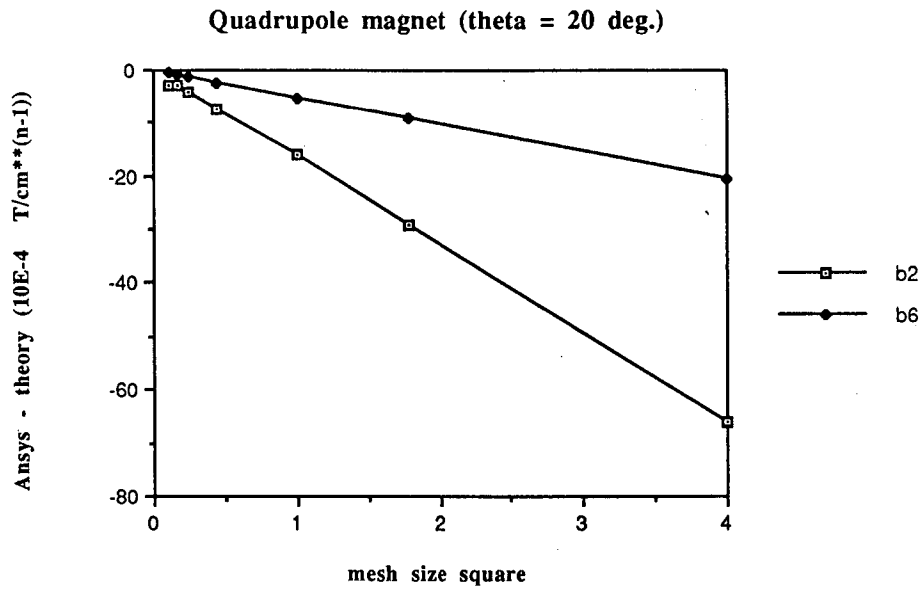


Fig. 13. Multipole coefficients versus mesh size for the quadrupole with  $\theta=20^\circ$ .

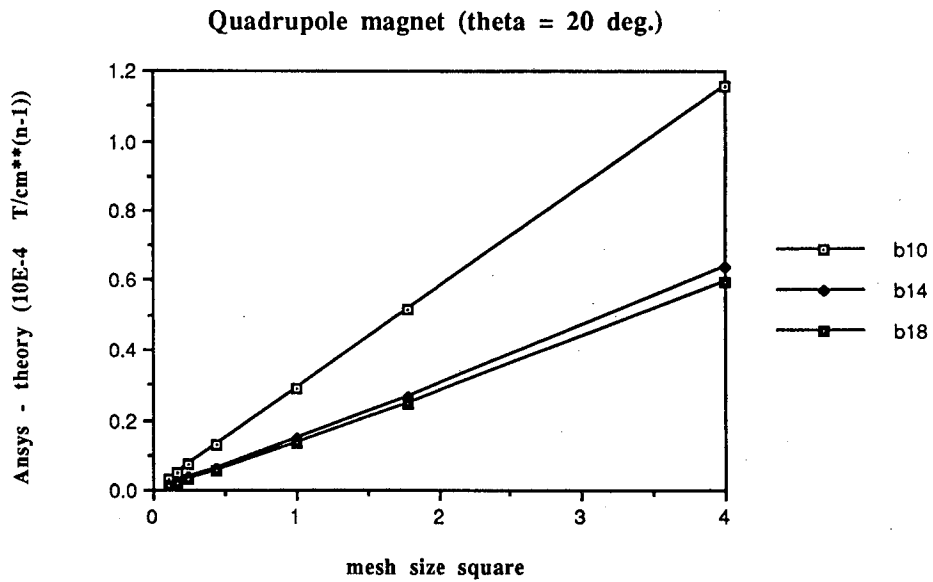


Fig. 14. Multipole coefficients versus mesh size for the quadrupole with  $\theta=20^\circ$ .

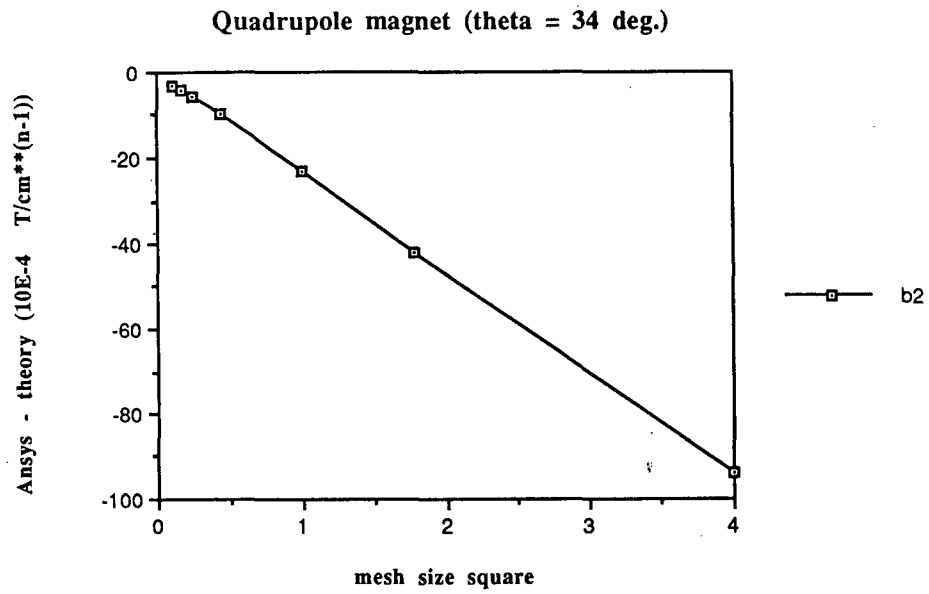


Fig. 15. Multipole coefficients versus mesh size for the quadrupole with  $\theta=34^\circ$ .

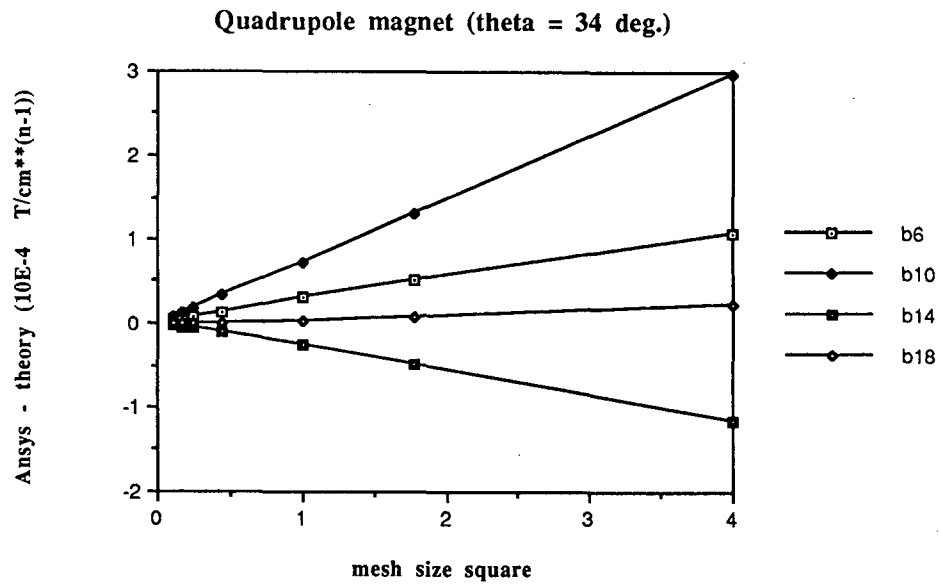


Fig. 16. Multipole coefficients versus mesh size for the quadrupole with  $\theta=34^\circ$ .

1/size	0.5	.75	1.0	1.5	2.0	2.5	3.	theory
b1	7.75329	7.75220	7.75183	7.75155	7.75145	7.75141	7.75139	7.75133
b3	0.59793E-1	0.60321E-1	0.605050E-1	0.60637E-1	0.60683E-1	0.60704E-1	0.60716E-1	0.60742E-1
b5	-0.21801E-1	-0.22694E-1	-0.23007E-1	-0.23230E-1	-0.23308E-1	-0.23344E-1	-0.23364E-1	-0.23409E-1
b7	0.12097E-2	0.13539E-2	0.14052E-2	0.14421E-2	0.14551E-2	0.14611E-2	0.14643E-2	0.14718E-2
b9	0.23159E-3	0.23106E-3	0.23119E-3	0.23138E-3	0.23146E-3	0.23149E-3	0.23151E-3	0.23157E-3
b11	-0.47381E-4	-0.53917E-4	-0.56875E-4	-0.59179E-4	-0.60029E-4	-0.60425E-4	-0.60642E-4	-0.61143E-4
b13	-0.48076E-4	-0.21021E-4	-0.11271E-4	-0.41980E-5	-0.17069E-5	-0.54658E-6	0.85348E-7	0.15200E-5
b15	-0.60567E-5	-0.15550E-5	-0.82721E-7	0.94349E-6	0.12867E-5	0.14518E-5	0.15361E-5	0.17346E-5
b17	0.56794E-5	0.270997E-5	0.14565E-5	0.50410E-6	0.15008E-6	-0.87667E-8	-0.20184E-6	-0.30177E-6
elements	1728	3888	6912	15552	27648	43200	62208	
cpu time (s)	96	227	445	1281	2976	6147	13464	

Table 1: Multipole coefficients versus mesh size for the dipole magnet ( $\theta = 56^\circ$ )

1/size	0.5	.75	1.0	1.5	2.0	2.5	3.	theory
b1	7.75329	7.75221	7.75183	7.75155	7.75146	7.75141	7.75139	7.75133
b3	0.59796E-1	0.60324E-1	0.60508E-1	0.60639E-1	0.60685E-1	0.60706E-1	0.60718E-1	0.60742E-1
b5	0.217970E-1	-0.22691E-1	-0.23003E-1	-0.23227E-1	-0.23305E-1	-0.23341E-1	-0.23361E-1	-0.23409E-1
b7	0.11976E-2	0.13468E-2	0.13999E-2	0.14381E-2	0.14515E-2	0.14577E-2	0.14611E-2	0.14718E-2
b9	0.21538E-3	0.22170E-3	0.22425E-3	0.22617E-3	0.22685E-3	0.22717E-3	0.22735E-3	0.23157E-3
b11	-0.64333E-4	-0.5750E-4	-0.55763E-4	-.54721E-4	-0.54393E-4	-0.54259E-4	-0.54172E-4	-0.61143E-4
b13	-0.67143E-4	-0.24807E-4	-0.96843E-5	0.12196E-5	0.50597E-5	0.68384E-5	0.78073E-5	0.15200E-5
b15	-0.65452E-5	-0.20432E-5	-0.54692E-6	0.46514E-6	0.81764E-6	0.97319E-6	0.10600E-5	0.17346E-5
b17	0.61454E-5	0.24180E-5	0.92735E-6	-0.22554E-6	-0.63467E-6	-0.832830E-6	0.636248E-6	-0.30177E-6
elements	1728	3888	6912	15552	27648	43200	62208	
cpu time (s)	107	250	479	1324	3016	6019	10882	

Table 2: Multipole coefficients versus mesh size for the dipole magnet ( $\theta = 56^\circ$ ) and automatic meshing

1/size	b2	b6	b10	b14	b18	elements	cpu time (s)
0.5	1.7201	0.11588E-1	0.91391E-5	0.54687E-4	0.59585E-4	1728	96
0.75	1.7238	0.12728E-1	-0.55053E-4	0.17564E-4	0.24539E-4	3888	226
1.0	1.7251	0.13127E-1	-0.77582E-4	0.53763E-5	0.13446E-4	6912	441
1.5	1.7260	0.13413E-1	-0.93652E-4	-0.28836E-5	0.58456E-5	15552	1273
2.0	1.7263	0.13513E-1	-0.99271E-4	-0.56676E-5	0.32612E-5	27648	2967
2.5	1.726453	0.13559E-1	-0.10187E-3	-0.69365E-5	0.20799E-5	43200	6170
3.0	1.726452	0.13584E-1	-0.10328E-3	-0.76189E-5	0.14395E-5	62208	13517
theory	1.72672	0.13641E-1	-0.10649E-3	-0.91571E-5	-0.83048E-22		

Table 3: Multipole coefficients versus mesh size for the quadrupole magnet ( $\theta = 20^\circ$ )

1/size	b2	b6	b10	b14	b18	elements	cpu time (s)
0.5	2.481	-0.6299E-2	0.1909E-3	-0.1060E-3	0.2267E-4	1728	104
0.75	2.486	-0.6356E-2	0.2382E-4	-0.3918E-4	0.6653E-5	3888	228
1.0	2.488	-0.6377E-2	-0.3360E-4	-0.1763E-4	0.2965E-5	6912	447
1.5	2.490	-0.6393E-2	-0.7422E-4	-0.2928E-5	0.9001E-6	15552	1316
2.0	2.490	-0.6399E-2	-0.8837E-4	0.2061E-5	0.3123E-6	27648	3000
2.5	2.490	-0.6402E-2	-0.9490E-4	0.4345E-5	0.6975E-7	43200	6202
3.0	2.490	-0.6403E-2	-0.9844E-4	0.5577E-5	-0.5746E-7	62208	13579
theory	2.491	-0.6407E-2	-0.1065E-3	0.8357E-5	-0.3225E-6		

Table 4: Multipole coefficients versus mesh size for the quadrupole magnet ( $\theta = 34^\circ$ )



## APPENDIX

Routine to perform the Fourier analysis of the magnetic field in a n-pole magnet.

This routine that runs on ANSYS 4.4A requires to have nodes on the circumference  $r=\text{arg1}$ , to specify the considered fraction (in the examples shown it is 1/4) of the magnet cross section and to use the MKS system.

```
*create,intg
/com THIS ROUTINE COMPUTES THE NORMAL MULTIPOLE COEFFICIENTS OF THE
/com MAGNETIC FIELD IN A N-POLE MAGNET
/com
/com Authors: Domenico Dell'Orco & Yanping Chen
/com          Lawrence Berkeley Laboratory
/com          1 Cyclotron road M.S. 46-161
/com          Berkeley, CA 94709
/com          USA
/com telephone (USA): (415)-486-7226
/com
/com IMPORTANT: only the allowed normal multipoles are correct.
/com
b1=0 $b2=0 $b3=0 $b4=0 $b5=0 $b6=0
b7=0 $b8=0 $b9=0 $b10=0 $b11=0 $b12=0
b13=0 $b14=0 $b15=0 $b16=0 $b17=0 $b18=0

csys,1
dsys,1
ra=arg1          * the multipoles are computed at the radius arg1
fr=arg2          * arg2 is the fraction of the magnet cross section
pi=4.*atan(1.)  * (1/2, 1/4...)
rcm=(ra*100)    * radius in cm
nset,x,ra
enode
ite=1
nelem
nrset,x,ra
nsort,y,1
*get,yml,min
nrset,y,yml,yml
*get,n1,ndmx
:la2
*if,ite,eq,1,:la1
n1=n2
yml=ym2
:la1
nelem
nrset,x,ra
nuset,y,0,yml
*get,mx,ndmx $*get,mn,ndmn
dn=(mx-mn)
nsort,y,1
*get,ym2,min
nrset,y,ym2,ym2
*get,n2,ndmx
/com          COMPUTE THE MULTIPOLE COEFFICIENTS bn
nset,,n1
naset,,n2
*get,ma1,mag,n1 $*get,ma2,mag,n2
*get,te1,y,n1 $*get,te2,y,n2
te1=(te1/180) $te1=(te1*pi)
te2=(te2/180) $te2=(te2*pi)
dc1=(cos((1*te2))-cos((1*te1)))
dc2=(cos((2*te2))-cos((2*te1)))
dc3=(cos((3*te2))-cos((3*te1)))
dc4=(cos((4*te2))-cos((4*te1)))
dc5=(cos((5*te2))-cos((5*te1)))
dc6=(cos((6*te2))-cos((6*te1)))
dc7=(cos((7*te2))-cos((7*te1)))
```

```

dc8=(cos((8*te2))-cos((8*te1)))
dc9=(cos((9*te2))-cos((9*te1)))
dc10=(cos((10*te2))-cos((10*te1)))
dc11=(cos((11*te2))-cos((11*te1)))
dc12=(cos((12*te2))-cos((12*te1)))
dc13=(cos((13*te2))-cos((13*te1)))
dc14=(cos((14*te2))-cos((14*te1)))
dc15=(cos((15*te2))-cos((15*te1)))
dc16=(cos((16*te2))-cos((16*te1)))
dc17=(cos((17*te2))-cos((17*te1)))
dc18=(cos((18*te2))-cos((18*te1)))
dma=(ma2-ma1)
dte=(te2-te1)
dmdt=dma/dte
b1=(b1+(dmdt*dc1))      $b2=(b2+(dmdt*dc2))
b3=(b3+(dmdt*dc3))      $b4=(b4+(dmdt*dc4))
b5=(b5+(dmdt*dc5))      $b6=(b6+(dmdt*dc6))
b7=(b7+(dmdt*dc7))      $b8=(b8+(dmdt*dc8))
b9=(b9+(dmdt*dc9))      $b10=(b10+(dmdt*dc10))
b11=(b11+(dmdt*dc11))   $b12=(b12+(dmdt*dc12))
b13=(b13+(dmdt*dc13))   $b14=(b14+(dmdt*dc14))
b15=(b15+(dmdt*dc15))   $b16=(b16+(dmdt*dc16))
b17=(b17+(dmdt*dc17))   $b18=(b18+(dmdt*dc18))
*if,dn,eq,0,:la3
ite=ite+1
*go,:la2
:la3
nall
cof=100                      * convert mag. potential from T*m to T*cm
cof=((cof/fr)/pi)
b1=((b1*cof)/1)              $b1=(b1/rcm**1)           * dipole
b2=((b2*cof)/2)              $b2=(b2/rcm**2)           * quadrupole
b3=((b3*cof)/3)              $b3=(b3/rcm**3)           * sextupole
b4=((b4*cof)/4)              $b4=(b4/rcm**4)           * octupole
b5=((b5*cof)/5)              $b5=(b5/rcm**5)           * decapole
b6=((b6*cof)/6)              $b6=(b6/rcm**6)           * 12-pole
b7=((b7*cof)/7)              $b7=(b7/rcm**7)           * 14-pole
b8=((b8*cof)/8)              $b8=(b8/rcm**8)           * 16-pole
b9=((b9*cof)/9)              $b9=(b9/rcm**9)           * 18-pole
b10=((b10*cof)/10)           $b10=(b10/rcm**10)        * 20-pole
b11=((b11*cof)/11)           $b11=(b11/rcm**11)        * 22-pole
b12=((b12*cof)/12)           $b12=(b12/rcm**12)        * 24-pole
b13=((b13*cof)/13)           $b13=(b13/rcm**13)        * 26-pole
b14=((b14*cof)/14)           $b14=(b14/rcm**14)        * 28-pole
b15=((b15*cof)/15)           $b15=(b15/rcm**15)        * 30-pole
b16=((b16*cof)/16)           $b16=(b16/rcm**16)        * 32-pole
b17=((b17*cof)/17)           $b17=(b17/rcm**17)        * 34-pole
b18=((b18*cof)/18)           $b18=(b18/rcm**18)        * 36-pole
*stat                      * display all (!) the parameters
*end
*use,intg,0.01,0.25      *arg1=radius   arg2=cross section fraction

```

LAWRENCE BERKELEY LABORATORY  
UNIVERSITY OF CALIFORNIA  
INFORMATION RESOURCES DEPARTMENT  
BERKELEY, CALIFORNIA 94720